

Journal of Materials Chemistry B

Accepted Manuscript



This is an *Accepted Manuscript*, which has been through the Royal Society of Chemistry peer review process and has been accepted for publication.

Accepted Manuscripts are published online shortly after acceptance, before technical editing, formatting and proof reading. Using this free service, authors can make their results available to the community, in citable form, before we publish the edited article. We will replace this *Accepted Manuscript* with the edited and formatted *Advance Article* as soon as it is available.

You can find more information about *Accepted Manuscripts* in the [Information for Authors](#).

Please note that technical editing may introduce minor changes to the text and/or graphics, which may alter content. The journal's standard [Terms & Conditions](#) and the [Ethical guidelines](#) still apply. In no event shall the Royal Society of Chemistry be held responsible for any errors or omissions in this *Accepted Manuscript* or any consequences arising from the use of any information it contains.

Polymeric Multifunctional Nanomaterials for Theranostics

Haisheng Peng^{1,2, †}, Xiaoying Liu^{2, †}, Guangtian Wang^{2, †}, Minghui Li², Kaitlin M. Bratlie^{1,3}, Eric Cochran¹, Qun Wang^{1,*}

¹*Department of Chemical and Biological Engineering, Iowa State University, Ames, IA 50011, United States*

²*Department of Pharmaceutics, Daqing Campus, Harbin Medical University, 1 Xin Yang Road Daqing, 163319, China*

³*Department of Materials Science and Engineering, Iowa State University, Ames, IA 50011, United States*

*Corresponding author:

Qun Wang, Ph.D.

Department of Chemical and Biological Engineering
Iowa State University
2114 Sweeney Hall
Ames, Iowa 50011
United States
Office: (515) 294-4218
Fax: (515) 294-8216
E-mail: qunwang@iastate.edu

† These authors contributed equally to this work.

Abstract: The nanocarriers provide a platform to integrate therapy and diagnostics, which is an emerging direction in medical practice. Beyond simply therapeutic functionality, theranostic nanomaterials have been designed to deliver multiple components and imaging agents, facilitating simultaneous and synergistic diagnosis and therapies. In this article, polymeric materials with diverse functionalities and properties for manufacturing theranostic nanomaterials are discussed and compared. We focused on recent advancements of polymeric multifunctional nanomaterials for synergistic theranostics. The drugs and imaging agents were encapsulated within and/or conjugated to the surface of the nanocarriers, according to the fabricating process and carrier type. In parallel with therapy, polymeric multifunctional nanomaterials can be exploited to exhibit distinctively magnetic, electrical, and optical properties for concomitant imaging. This has been accomplished by incorporating various imaging agents, such as fluorescent dyes, biomarkers, quantum dots, metal composites, and magnetic nanoparticles. We discussed theranostic nanomaterial synthesis, carrier fabrication and its applications. By presenting this comprehensive review of the state-of-the-art, we demonstrated that polymeric multifunctional nanomaterials exhibit distinctive advantages and features in theranostics.

Key Words: Polymeric; Multifunctional; Nanomaterials; Theranostics

TABLE OF CONTENTS

1. Introduction
2. Drug-polymer conjugates
3. Nanoparticles
 - 3.1 Solid lipid nanoparticles
 - 3.2 Dendrimers
 - 3.3 Liposomes
 - 3.4 Polymeric micelles
4. Nanocomposites
 - 4.1 Polymeric/magnetic nanoparticles
 - 4.2 Polymeric/silica nanoparticles
 - 4.3 Polymeric/gold nanoparticles
 - 4.4 Polymeric/quantum dots
 - 4.5 Polymeric nanoparticles
5. Application of theranostic nanoparticles in diseases
 - 5.1 Cancer
 - 5.2 Cardiovascular diseases
 - 5.3 Kidney diseases
 - 5.4 Pulmonary diseases
 - 5.5 Inflammatory diseases
 - 5.6 Neurodegenerative diseases
6. Clinical trial and market
7. The current challenges and prospect

1. Introduction

Nanocarriers provide a platform for theranostics to concurrently realize therapy and diagnosis¹. Polymeric drug delivery systems have been widely studied for years. In the 1960s, polymers were mainly utilized for wound healing, blood plasma expanding, and injectable drug releasing^{2, 3}. Normally, polymeric nanoparticles are used to deliver drugs to affected tissues and to regulate the release kinetics of the drugs in the body. Prior to treatment, clinical diagnosis is an essential step. Recently, researchers are aiming to achieve diagnosis and therapy in one combined step. Clinicians may monitor drug localization and image the result of the treatment simultaneously after drug administration.

Advances in nanotechnology significantly influenced the treatment and detection of diseases⁴⁻⁷. The strategies used in advanced theranostics, such as polymer conjugations, solid lipid nanoparticles, dendrimers, micelles, magnetic nanoparticles, silica nanoparticles, and quantum dots, may achieve fewer side effects and better synergistic outcomes^{8, 9}. The goal of theranostics is to diagnose and treat a disease at its earliest stage. Advanced theranostic nanomedicine possessing multifunctional properties in nature has the ability to diagnose and deliver therapy to the diseased cells with the help of biomarkers and targeting ligands¹⁰⁻¹³. Conjugation, entrapment, absorption, and encapsulation of drugs and diagnostic agents in polymeric particles can result in combined loading, ultimately achieving the function of theranostics at the molecular and cellular levels¹⁴⁻¹⁶.

The therapeutic agents used in theranostic nanomedicine include small chemicals, genetic materials, proteins, and peptides. Imaging techniques that are used in theranostics are mainly dependent on the contrast agent used¹⁷. As a 2D imaging instrument, gamma scintigraphy is more efficient in visualizing drug localization through pulmonary and oral routes. As a 3D imaging system, positron emission tomography (PET) and single photon emission computed tomography (SPECT) can be used to observe regional depositions of drugs in the lung. However, some practical hurdles limit the clinical application of SPECT and PET¹⁸. In order to deliver active drugs and imaging agents simultaneously, drug delivery systems (DDS) have been designed to control therapeutic agents' release to treat illnesses and to mark the

affected tissues or cells. For specific conditions like hypoxia, the control of pH, temperature, light, and ultrasound has been carried out to precisely regulate the pharmacokinetics of the drugs and imaging agents^{19,20}. Contrast agents in DDS can also be used to monitor the accumulation of particles in tissues and to observe the interactions between the carriers and the microenvironment through a non-invasive way. In this review, we summarize the recent developments in multifunctional polymeric nanomaterial theranostic platforms, for instance drug-polymer conjugates, solid lipid nanoparticles, dendrimers, micelles, magnetic nanoparticles, silica nanoparticles, polymeric/magnetic nanoparticles, polymeric/silica nanoparticles, and quantum dots^{21,22}. We hope that this review can provide a broad overview of the scope of multifunctional polymeric nanomaterials in theranostics.

2. Drug-polymer conjugates

Polymers with long chain molecules are linked by covalent bonds and can be used to regulate the pharmacokinetics of drugs and/or imaging agents in the body. Drug-polymer conjugates are formed through the connection of various functional groups between the polymer and the drug or imaging agents, providing real-time observations on the localization and delivery efficiency of the conjugates. For example, tumor angiogenesis promotes the growth of malignant cells. The arginine-glycine-aspartic (RGD) sequence can interact with $\alpha_v\beta_3$ integrins and direct the targeted delivery of nanocarriers to tumor vessels, enhancing their accumulation in tumor tissues. Yuan *et al.* synthesized poly [N-(2-hydroxypropyl) methacrylamide (HPMA)-c (RGDyK)-1, 4, 7, 10-tetraazacyclododecane-1, 4, 7, 10-tetraacetic acid] (DOTA)-⁶⁴Cu copolymers and evaluated the *in vivo* tumor localization of theranostic scaffolds by PET. The RGD sequence enhanced the radioactivity of the copolymer in prostate cancer xenografts from 1.29% \pm 0.26% injected dose (ID)/g to 2.75% \pm 0.34% ID/g (2.13 fold). The data showed that the copolymer could potentially be used to prepare new nanocarriers for tumor imaging and radiochemotherapy²³.

Similarly, Zarabi *et al.* replaced Cu with Gd and found that the polymeric conjugates possessed

stronger relaxivities than that of Gd-DOTA. Conjugation did not impact the affinity of RGD for $\alpha\beta_3$ integrins on endothelial cells and MDA-MB-231 breast cancer cells²⁴. The RGD sequence plays another vital role in the targeted delivery of nanocarriers. Mitra *et al.* compared the localization of HPMA-technetium-99m-RGD4C (sequence: KACDCRGDCFCG) and HPMA-technetium-99m (99mTc(CO)3)-RGD4E (KACDCRGEFCG) at the sites of neovascular angiogenesis and found that the scintigraphic images showed higher biodistribution of the former conjugates, based on the radioactivity²⁵. However, the chelator of 99mTc(CO)3 (N-L-bis(2-pyridylmethyl)-L-lysine (RGD4C-DPK)) decreased the accumulation of conjugates to some extent²⁶. Poly(L-glutamic acid) is another candidate for diagnosis and therapeutics. Ye *et al.* connected poly(L-glutamic acid) with 1,6-hexanediamine-(Gd-DO3A) and observed the influence of molecular weight on the conjugates' pharmacokinetics. The data from contrast enhanced Magnetic Resonance Imaging (MRI) showed that the copolymer with the smallest molecular weight (28 kDa) was most rapidly removed from the body, with the lowest tumor accumulation. On the contrary, other larger molecules (87 and 50 kDa) improved blood circulation times and exhibited stronger signals in the tumor tissues²⁷ (Fig. 1).

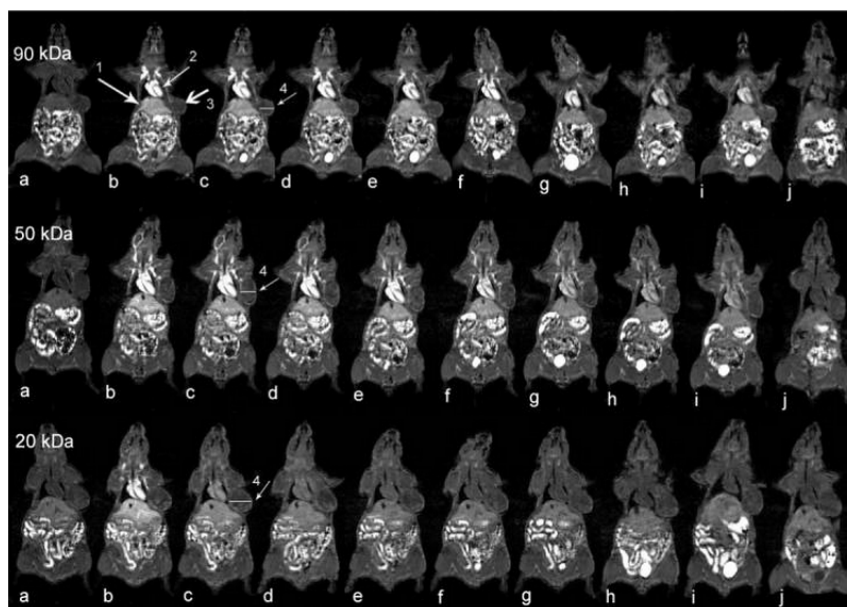


Fig. 1 Representative coronal images of mice organs and xenografts by MR after intravenous administration of PGA-1,6-hexanediamine-(Gd-DO3A). Time points for images are: (a) before tests, (b) 1 min, (c) 11 min, (d) 20 min, (e) 30 min, (f) 60 min, (g) 120 min, (h) 180 min, (i) 240 min and (j) 24 h. Arrows: (1) liver, (2) heart, (3) tumor tissue, and signal intensity of (4) cross-section in tumor tissue (reprinted with permission from ref. 27).

3. Nanoparticles

Nanoparticles are a category of nanoscale carriers based on polymers for drug delivery and diagnosis. These nanoscale particulates may consist of multiple functional units. They have been extensively employed to control the delivery of encapsulated drugs and imaging agents for both diagnosis and therapy.

3.1. Solid lipid nanoparticles

Solid lipid nanoparticles (SLNs) are DDS with improved stability compared with nanoparticles, liposomes, and emulsions. SLNs possess other advantages such as controlled release, targeted delivery, and high loading efficiency while avoiding the use of organic solvents^{28,29}. The dissolved or dispersed drug exists in the solid hydrophobic core, while excipients, including surfactants and phospholipids, are generally recognized as safe for clinical therapy. However, the drawbacks of SLNs, such as size growth, burst release at the earlier stages, tendency of uncontrollable gelation, and dynamics of polymeric transitions, limit their application³⁰. Several methods for SLN preparation have been published, including high speed/pressure homogenization^{31, 32}, double emulsion³³, ultrasound dispersion³⁴, and use of membrane contactors^{35,36}. Similar to other nanomaterials, SLNs can be used as theranostic formulations to deliver therapeutic and diagnostic agents to targeted sites.

Drugs cannot effectively accumulate in tumor tissues through conventional administration routes. Lymphatic delivery of SLNs can enhance the bioavailability of drugs after oral administration³⁷. Reddy *et al.* prepared solid lipid tripalmitin nanoparticles labeled with ^{99m}Tc and containing etoposide. They evaluated the biodistribution and tumor uptake of nanocarriers in mice through subcutaneous, intravenous,

and intraperitoneal injection. The data showed that subcutaneous injection decreased the biodistribution of nanoparticles in all organs. Moreover, intraperitoneal administration increased the accumulation of particles in tissues compared with that observed after delivery of free drug via the same route and intravenous administration. However, nanoparticles accumulated in the tumor in a slower and more progressive way after subcutaneous administration, and the accumulation was significantly higher than that induced by intravenous (59 fold) or intraperitoneal injection (8 fold) 24 h after administration³⁸. Similarly, Cavalli *et al.* confirmed that SLNs containing taurocholate, stearic acid, and phosphatidylcholine increased the absorption of tobramycin after duodenal administration and extended the half time of the drug in blood from 57 min (free drug) to 1371 min (drug in SLNs)³⁹.

Bae *et al.* entrapped low-density lipoprotein (LDL), paclitaxel, and quantum dots (QDs) into SLNs (PQSLNs) and decorated their surface with siRNA. The particles efficiently delivered anti-cancer drugs and oligonucleotides into lung cancer cells. The data confirmed that siRNA could promote the anti-cancer activities of paclitaxel in a synergistic way. The fluorescent signal obtained from the quantum dots in the SLNs enabled the visualization of the intracellular trafficking of particles in the cells. The results suggested that SLNs can be used as a multifunctional platform to efficiently treat cancers (Fig. 2)⁴⁰.

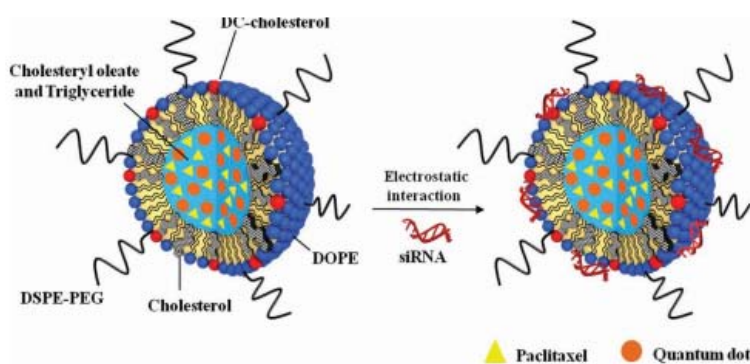


Fig. 2 Schematic of PQSLNs, as a theranostic formulation, entrapping quantum dot and paclitaxel and coated with siRNA on the surface of nanoparticles to treat cancer in a synergistic way (reprinted with permission from ref. 40).

3.2. Dendrimers

The elementary structure of dendrimers presents a tree-like branched architecture, providing room for a small molecule to be incorporated⁴¹. Dendrimers, as nanocarriers, have tunable nanoparticle sizes from 10 to 100 nm. They are able to solubilize hydrophobic drugs because of their unique structure. The higher generation dendrimers with a number of branches and cavities are able hold dyes, small molecules, diagnostic agents, and other therapeutics for theranostic applications. Dendrimers were used to load cisplatin for cancer treatment and was proven to have a stronger effect on the malignant cells⁴². The monodispersed macromolecules on the surface of the dendrimers possess a few reactive end groups to modify the properties of the carriers. Weck's group designed a multifunctional dendrimer based on polyamine. The active end groups of the dendrimers included nine amines, nine azides, and 54 acids, connecting with a near-infrared (NIR) cyanine dye. This new material exhibited no toxicity to human glioblastoma cells (T98G) and might be a promising material for theranostics (Fig. 3)⁴³.

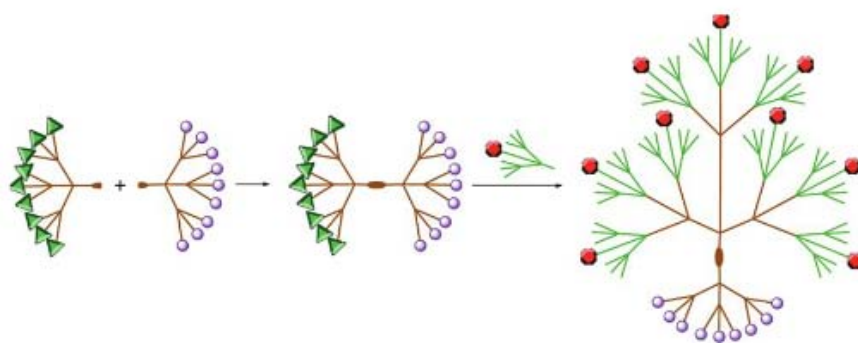


Fig. 3 Advanced dendrimer with functional termini, including NIR fluoresceins, acidic acid, and azide groups for connection with therapeutics or imaging reagents (reprinted with permission from ref. 43).

Phthalocyanines are excellent dyes that can be excited to produce near-infrared (NIR) light. This dye is believed to be a theranostic agent to monitor the biodistribution of nanoparticles for the treatment of deep tumors. However, the dye has hydrophobic properties, high aggregation, and low specificity to cancer cells, and therefore, it cannot be used to efficiently treat cancer in clinic applications. Taratula *et al.* synthesized novel polypropylenimine dendrimer carriers to deliver phthalocyanines into tumors. The dye

was modified with a hydrophobic molecule to increase the encapsulation efficiency in the dendrimer while luteinizing hormone-releasing hormone (LHRH) and poly (ethylene glycol) (PEG) surface coating of the carriers enhanced the biocompatibility and targeted delivery of the dye. The *in vivo* imaging studies confirmed that the dendrimer improved the localization of the dye in the tumor tissues after intravenous injection⁴⁴.

Radiovirotherapy is a method to use viruses to deliver radioisotopes into the body; it is another strategy to eradicate tumors. Grünwald *et al.* coated adenovirus that was inserted with the gene of the theranostic sodium-iodide symporter using cationic poly (amidoamine) (PAMAM) dendrimers. In addition, the dendrimer was decorated with specific ligand GE11 of epidermal growth factor receptor (EGFR) to direct the delivery of transfected adenovirus to tumor sites. At fourth day of intravenous adenovirus injection, mice were injected intraperitoneally with 18.5 MBq ¹²³I, and radioiodine accumulation was scanned with gamma camera imaging equipment. The high expression of sodium-iodide symporter in the tumor by targeted delivery of the dendrimers enhanced the accumulation of ¹²³I and promoted the killing effects of radioiodine on the malignant cells. The competitive affinity of EGFR-specific antibodies significantly reduced the biodistribution of ¹²³I in the tumor tissues, which supported that EGFR, and not coxsackie-adenovirus receptors, conferred the targeting function of the carriers. The existence of adenovirus in the liver was reduced by its shielding and targeting with EGFR specific ligand GE11-coated dendrimers, which protected the healthy liver from high exposure of radioiodine and increased the transduction efficiency in tumor tissues (Fig. 4)⁴⁵.

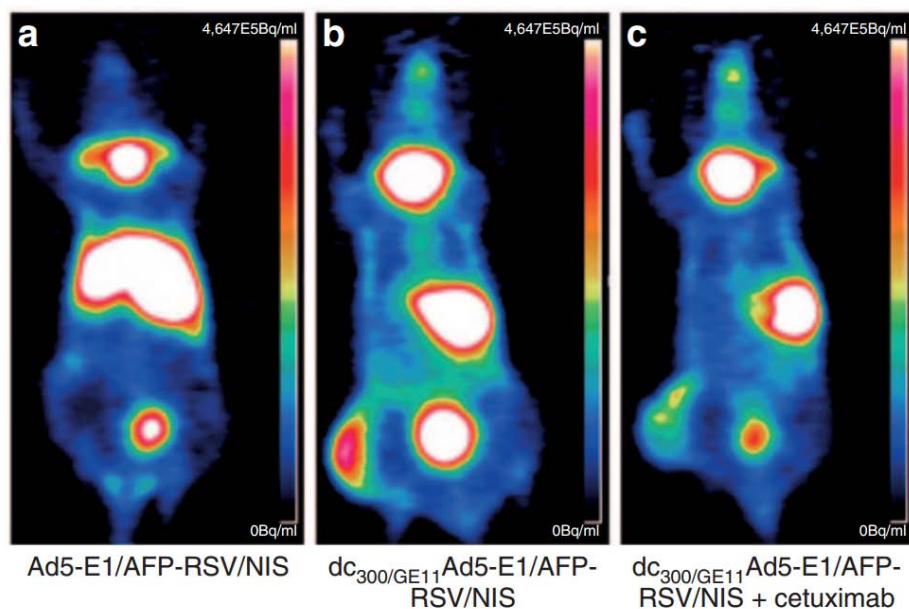


Fig. 4 The *in vivo* images of EGFR-specific accumulation by ^{124}I -PET tracking. (a) The uncoated vector had high hepatic accumulation after administration showed in the middle with larger area (i.v.). (b) Adenovirus coated with PAMAM-G2-PEG-GE11 showed in the middle with larger area or (c) monoclonal anti-EGFR antibodies decreased radioiodine accumulation in the liver showed in the middle with larger area (reprinted with permission from ref. 45).

3.3. Liposomes

Liposomes are small bilayer vesicles with aqueous compartments enclosed by cholesterol and amphiphilic phospholipids. They constitute a nanotechnology-based drug delivery platform and are effective because of their size, characteristics, biodegradability, biocompatibility, immunogenicity, and low toxicity⁴⁶⁻⁴⁸. Liposomes have great potential applications in drug delivery, molecular imaging, vaccine delivery, and gene therapy^{16, 49-51} (Fig. 5). The disadvantages of liposomal vesicles are poor stability, low drug-loading efficiency, short circulation time in the blood, and fast drug release⁵². Liposomes could be easily removed by macrophages in the immune system. To overcome the drawbacks of these vesicles, modifying the surfaces of the liposomes with PEG turns them into stealth liposomes, inhibiting the removal of the vesicles by macrophages and increasing the stability of the carriers. Because of the inhibition of stealth liposomes by lymphatic drainage and the inherently leaky vasculature within tumor tissues, liposomes can passively accumulate in solid tumors and deliver drugs to destroy malignant cells. PEG chains can also be conjugated with molecular biomarkers to develop advanced theranostic

liposomes.

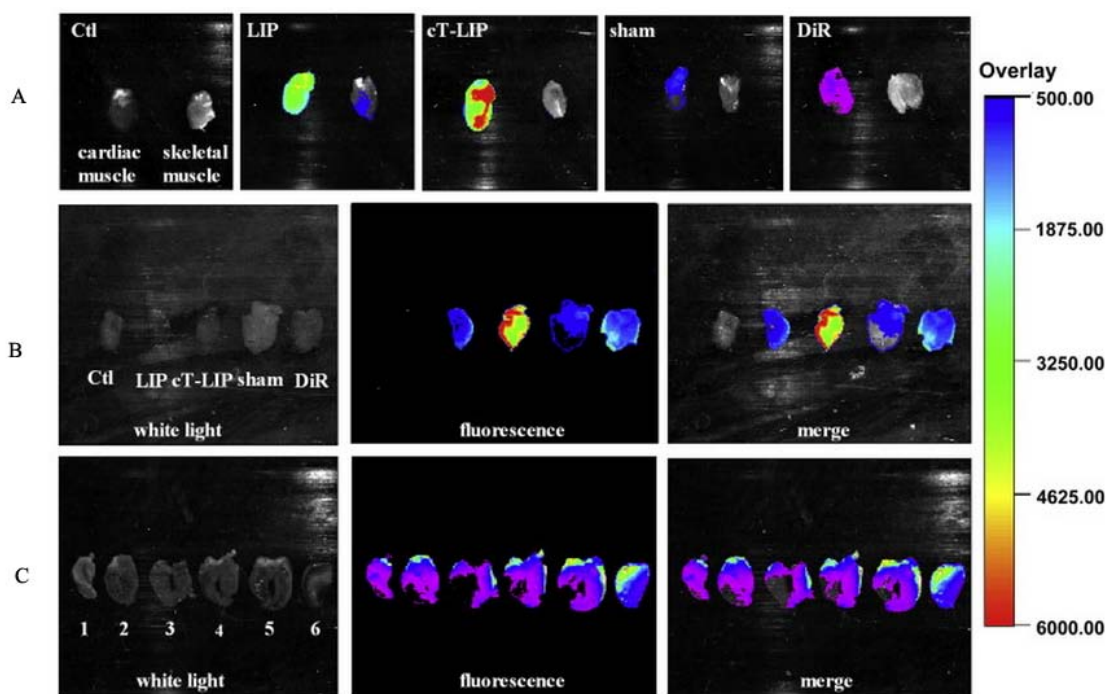


Fig. 5 (A) The *ex vivo* images of ischemic cardiac muscle and normal skeletal muscle 6 h after injection of cTnI antibody-modified liposomal 1, 1'-dioctadecyl-3, 3', 3'-tetramethylindotricarbocyanine iodide (DiR). (B) Fluorescence distribution of left ventricular sections from different animals administrated with PBS, unmodified liposomes, cTnI antibody-modified liposomes (cT-LIP), sham with cT-LIP, and free DiR groups. (C) Images of cardiac sections from animals injected with cT-LIP formulation (reprinted with permission from ref. 49).

Researchers have designed anti-HSP72 gene-transfected stealth immunoliposomes loaded with imaging probes to track themselves by using various types of imaging equipment. The vesicles were further loaded with citicoline to simultaneously improve the symptoms of cerebral ischemia. The data confirmed that the immunoliposomes (80%) were able to accumulate in the peri-infarct region after MRI observation. The lesion volume of rats after the injection of immunoliposomes was up to 30% smaller than that of free citicoline⁵³. Wen *et al.* incorporated apomorphine and quantum dots (QDs) into theranostic liposomes, resulting in decreased accumulation in the liver and increased the distribution in the brain⁵⁴. QDs in the bilayer membrane of the liposomes were used to image the distribution of vesicles in the brain, while the drug in the inner core of the vesicles was used to treat brain disorders. The data

confirmed that after liposomal administration, the signal of theranostic liposomes in the animal brain was higher than that of free QDs. The *ex vivo* imaging of the organs also supported the above-discussed *in vivo* results. However, the signals in the liver and heart were decreased after liposomal administration. Apomorphine in the brain was enhanced by 2.4-fold after this incorporation.

3.4. Polymeric micelles

Polymeric micelles are self-assembling colloidal structures with a hydrophilic shell and a hydrophobic core. They have properties such as appropriate size range (20–200 nm) for penetrating the blood vessels, high solubility and stability, and long circulation in the body⁵⁵. The strong associations between the polymers and the drug, as well as the conjugation of the polymeric core or of the shell improve the stability of the carriers. The localization of the loaded drug within the particles depends on the properties of the drug, such as polarizability and hydrophobicity. In addition, targeted micelles can prevent premature drug release in the body.

Kim *et al.* loaded doxorubicin (DOX) into folate-modified micelles and evaluated the therapeutic efficacy of the particles by *in vivo* studies. The growth of xenografts in nude mice, after administration of drug loaded pH sensitive micelles and non-sensitive micelles, was significantly delayed. However, free DOX was unable to inhibit the growth of tumor volume (an exponential growth curve). Monitoring of both micelles and free drug was carried out by intravital fluorescence microscopy from 0 to 60 min (0, 7, 10, 20, and 60 min). The fluorescence signal of free DOX could be observed from 7 to 60 min. At 60 min, the signal after the administration of the drug-loaded pH-sensitive micelles was still maintained, while that of the blank pH-sensitive micelles began to decrease. In another study, a micelle system used to load cyanine dye and doxorubicin as a novel theranostic platform possessed multiple functionalities such as thermotherapy, near-infrared fluorescence (NIRF) imaging, and synergistic chemotherapy of cytotoxicity from DOX and singlet oxygen from the dye to tumor cells. The results suggested that the micelles were used as a theranostic platform for multi-synergistic therapy and cancer imaging⁵⁶ (Fig. 6).

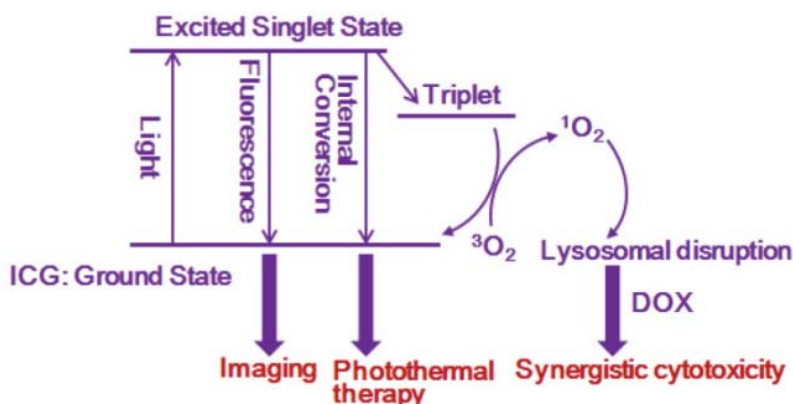


Fig. 6. Synergistic mechanism of cyanine-loaded micelles for cancer therapy (reprinted with permission from ref. 56).

4. Nanocomposites

Nanocomposites possess multifunctional properties and have many advantages for delivery of drugs and imaging agents. Nanocomposites can be modified with several ligands to achieve the goal of diagnosis, therapy, and entry of carriers across the tissue barrier⁵⁷. The ligands on the surface of nanocomposites enhance the binding affinity of the particles to the targeted cells. In the following part, multifunctional nanocomposites that carrying various targeting moieties for cancer therapy and diagnosis will be discussed.

4.1. Polymeric/magnetic nanoparticles

Polymeric/magnetic nanoparticles have been studied as theranostic platforms for various therapies⁵⁸. Magnetic nanoparticles are composed mainly of iron oxides made from magnetite or hematite⁵⁹. Magnetic iron oxide nanoparticles have found their way into different fields of medicine and can be synthesized by simple methods, including thermal decomposition and co-precipitation.

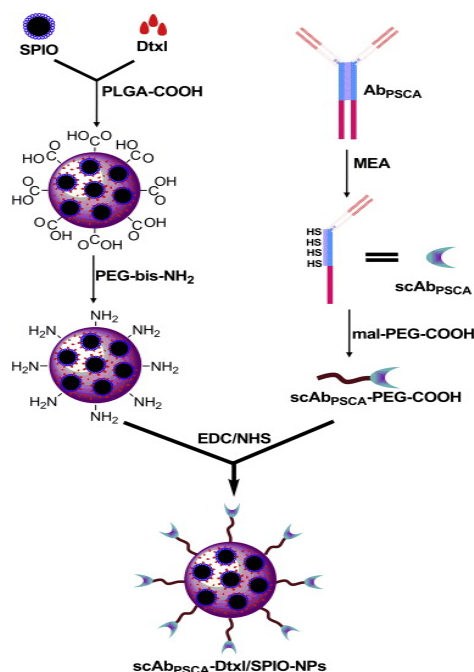


Fig. 7 Schematic process of scAbPSCA-docetaxel/SPIOs for prostate cancer (reprinted with permission from ref. 67).

Because of their magnetic properties and biocompatibility, superparamagnetic iron oxide nanoparticles (SPIONs) have been widely investigated. In MRI, SPIONs have been studied as T2 contrast agents. In addition, they have been used to deliver photodynamic therapeutic agents and chemical drugs as theranostics⁶⁰. The PEGylated SPIONs can improve colloidal stability and biocompatibility⁶¹. Chen et al. synthesized SPIONs and conjugated folic acid through PEG linker on their surface⁶². The SPIONs had good dispersibility and stability in various pH solutions. In addition, the clearance of SPIONs by macrophage was lower than superparamagnetic iron oxide associated with dextran (Feridex I.V.). SPIONs can also be coated with cell- or protein-resistant polymers such as poly(TMSMA-r-PEGMA) as MRI agents for *in vivo* cancer imaging⁶³. The modification of the antifouling polymer on the surface of SPION decreased the clearance of reticular endothelial system (RES) and elongated the circulating time of particles in the vessels. The synthesis of carbohydrate-coated SPIONs as MRI nanoprobes has also been designed to include the derivatives of D-mannose and D-glucosamine⁶⁴. Antibody-SPION conjugates can be synthesized via the ionic interactions between the nanoparticles and the antibody by using

immobilization methods. SPIONs coated with polymers were conjugated with antibodies to target human epithelial growth factor receptor 2 (HER-2) to enhance drug delivery to some HER2-overexpressed human cancer cells⁶⁵. Valero et al. employed the assembly-disassembly process of apoferritin proteins driven by pH to form magnetic nanoparticles and further modified the particles via the outer apoferritin with carbohydrates to enhance the targeting properties⁶⁴. In addition, aptamers are another candidate for the modification of SPIONs mixed with plasmonic Au^{65, 66}. After conjugated, the modified particles could be used to collect and detect various cancer cells. Ling *et al.* coated single chain anti-prostate stem cell antigen antibodies (scAb-PSCA) on the SPION surface for the treatment and imaging of prostate cancer⁶⁷ (Fig. 7). Prostate stem cell antigen (PSCA) is expressed in normal prostate cells and is overexpressed in prostate tumor cells⁶⁸. The scAb-PSCA served as a linker between SPIONs and docetaxel (Dtxl), and it was proven that the scAb-PSCA-Dtxl/SPIONs could be used as a real-time monitoring tool for the therapeutic effects and MRI contrast agents for prostate-targeted imaging. The cell-based systematic evolution of ligands by exponential enrichment (SELEX) strategies were used to scan the affinity of aptamers. The aptamers modified magnetic nanoparticles were used to extract the targeted cells while that conjugated with fluorescent particles to detect the cancer cells.

4.2. Polymeric/silica nanoparticles

Generally, mesoporous silica nanoparticles (MSNPs) consist of three primary components, including a solid support, a payload of cargo, and external machinery. MSNPs have been investigated as effective drug delivery systems for therapeutic agents against various diseases⁶⁹. It is easy to introduce various functional groups onto the nanoparticles by either electrostatic interactions or covalent bonding, conferring various mechanized features and high versatility to the mesoporous silica materials. As vehicles for the targeted delivery of γ -secretase inhibitors (GSIs), traceable MSNPs were used to block Notch signaling. Cell-specific Notch inhibition improved the premature leakage of the drug during its delivery. In detail, MSNPs loaded with GSIs were coated with polyethylenimine (PEI) and connected

with folic acid to target breast cancer cells. The *in vivo* data showed that the goal of the targeted delivery of MSNPs was realized to some extent (Fig. 8). Furthermore, most of the nanoparticles were eliminated *via* the renal pathway after degradation⁷⁰.

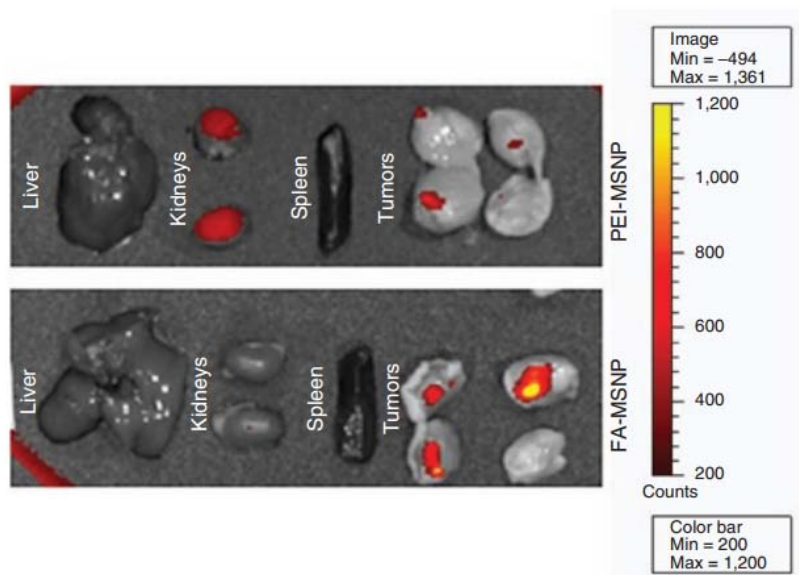


Fig. 8 The signal intensity of *ex vivo* organs (liver, kidney, and spleen) and tumors three days after injection of MSNPs. The xenografts were split in half to monitor the distribution of the particles in the tissues (reprinted with permission from ref. 70).

In another study, researchers compared the different photodynamic efficacies of silica nanoparticles containing phthalocyanine 4 (Pc4) (Pc4SNPs) and free Pc4 solution. Encapsulation of Pc4 into the polymeric nanoparticles can avoid fluorescent signal quench in the photodynamic therapy, as well as enhance therapeutic efficacy. After encapsulation, the fluorescence spectra and absorption of Pc4SNPs were blue-shifted, and the fluorescence intensity of Pc4SNPs was more enhanced than that of free Pc4 at the same absorbance. LysoTracker Green DND-26 or MitoTracker Green FM was used to mark the lysosomes and mitochondria of A375 and B16F10 cells, as well as colocalize Pc4SNP with these organelles. The results confirmed that compared with free Pc4, Pc4SNPs had higher accumulation in the mitochondria and lysosomes⁷¹.

4.3. Polymeric/gold nanoparticles

Gold nanoparticles (GNS) are versatile platforms that are highly valued as theranostic systems owing to their particular structures and attractive optical properties for photothermal therapy, such as near-infrared absorption, surface enhanced Raman scattering, and localized surface plasmon resonance^{72, 73}. The surface of GNS can be effortlessly functionalized with ligands and other functional chemotherapeutics⁷⁴. GNS with core sizes of less than 10 nm provide a large area for ligand modification and drug conjugation. They are usually synthesized using hydrogen tetrachloroaurate and have been widely investigated as drug carriers, radiosensitizers, photothermal converters, and imaging probes in a broad range of applications in cancer diagnosis and therapy⁷⁵. Researchers have shown that GNS have the potential to heighten the efficacy of conventional treatment modalities and are promising tools in diagnostic imaging, minimally invasive thermal ablation therapy, multimodal anti-cancer therapy, and intraoperative tumor margin delineation⁷⁶.

Heo *et al.* designed GNS functionalized with PEG, biotin, paclitaxel, and dye (rhodamine B)-linked cyclodextrin derivatives (beta-CD) to undertake therapy and diagnosis simultaneously⁷⁷. As a theranostic platform, beta-CD interacted with paclitaxel and the two formed an inclusion complex. Thereafter, cyclodextrin was connected to the oval GNS with size in the range of 20-40 nm. The *in vitro* studies indicated that GNS had a stronger targeting efficiency toward cancer cells such as HeLa, A549, and MG63 than toward NIH/3T3 cells. In addition, GNS possess significant cytotoxicity against HeLa cells. The preliminary study supported that GNS are feasible for use in theranostic nanomedicine. In another study, researchers utilized gold nanosphere (~33 nm) coated with tumor necrosis factor-alpha (Au-TNF) and heated by laser pulses⁷⁸ (Fig. 9). To enhance the photothermal efficiency, the researchers investigated the influence of nanoparticle structure on therapy and diagnosis. A murine carcinoma model was used to compare the therapeutic efficacies of laser with or without Au-TNF conjugates, Au-TNF conjugates alone, laser with TNF-free gold nanospheres, and Au-TNF alone. The results confirmed that the combination of laser with Au-TNF conjugates resulted in a stronger efficacy toward cancer cells. Currently, the photothermal activation of Au-TNF conjugates is in phase II trial in humans. The Au-TNF

conjugates can be combined with clinically relevant nanodrugs to acquire synergistic anti-tumor theranostic action.

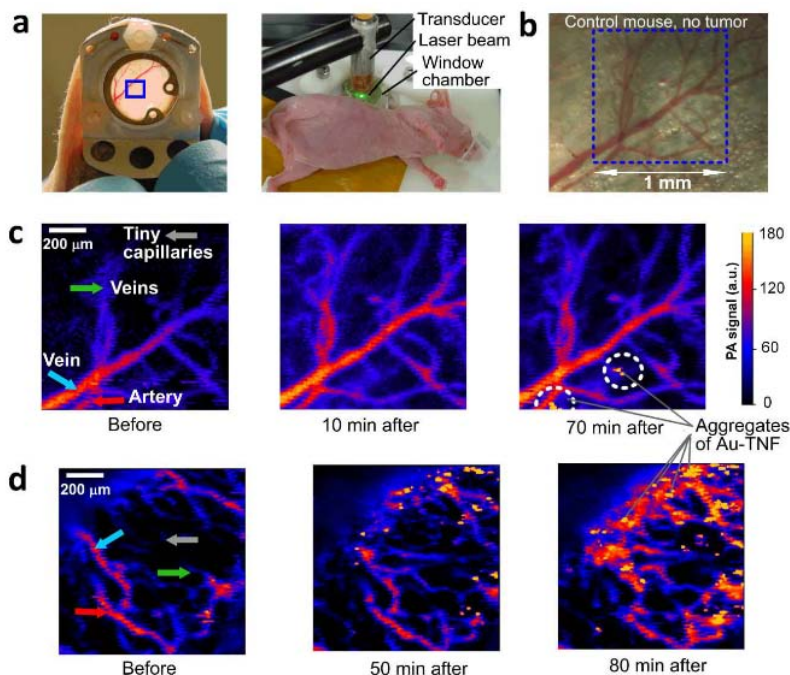


Fig. 9 Au-TNF penetration from ear vessels in mice. (a) Window chamber (left) and Photo-acoustic (PA) probe (right). (b) Healthy blood vessels. (c) Representative images of Au-TNF within healthy vessels and of (d) Au-TNF in the vessels within murine mammary cancer cells tumor before and after administration (i.v.) (reprinted with permission from ref. 78).

4.4. Polymeric/quantum dots

Quantum dots (QDs) were put forward as a new concept in the 1990s⁷⁹. They are nanocrystals made of semiconductor materials and have light-emitting properties that can be optimized by tuning their composition and size. Most QDs are made up of binary alloys of II-VI or III-V semiconductor materials. QDs are crystalline particles and the size of QDs ranges from 1 to 10 nm. QDs are often encapsulated in an insulating inorganic shell to increase the quantum yield. The coating materials on the surface of the ZnS-capped CdSe QD cores (less than 10 nm) protect it from the microenvironment. It was reported that QD-peptide conjugates accumulated in liver tumors⁸⁰ (Fig. 10). *Ex vitro* histological results confirmed

that the conjugates were able to target cancer in mice, and the PEG coating significantly lowered the reticuloendothelial clearance. However, *in vivo* detection of the QD signal is challenging.

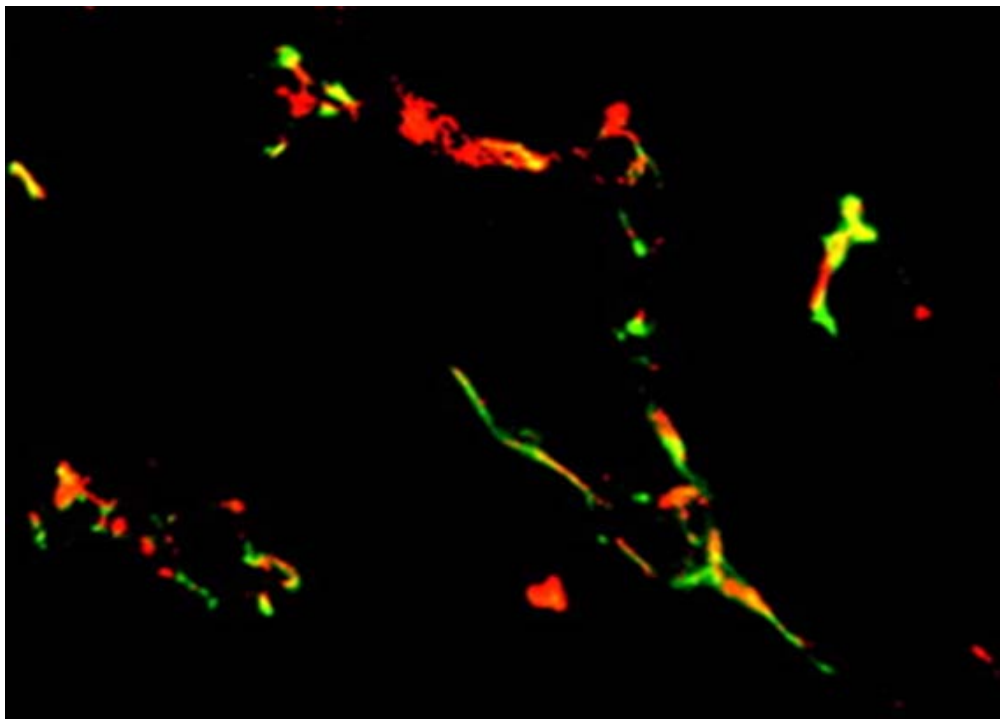


Fig. 10 The colocalization of F3 QDs with vascular tissues within xenograft (reprinted with permission from ref. 80).

For synchronous traceable drug delivery and cancer imaging, QD (CdSe/ZnS core-shell QD490)-aptamer (Apt)-DOX (QD-Apt-DOX) was developed as QD-based theranostics⁸¹. RNA aptamers were conjugated onto the diagnostic modality for therapeutic application. Drug sensing was designed on the basis of Förster resonance energy transfer (dual donor-quencher) in terms of drug release. When in the drug-loading state, the fluorescence of the QDs and the fluorescence of DOX were successively quenched by DOX and the aptamer, respectively. During drug release, DOX was liberated from the QD-Apt complexes to turn the fluorescence “ON”. The fluorescence of DOX was traced during drug transport. This multifunctional QD system heightened the therapeutic specificity against targeted LNCaP cells. The drug could be tracked by the fluorescence of Dox during its release and transport.⁸² In another study,

NIR-emitting CdTe QDs (~ 4.5 nm) were synthesized by attaching cyclicRGD (cRGD) peptides to the QDs' surface. *In vivo*, the margins of tumor and the tumor itself were visualized and distinguished by the resulted QDs. Moreover, the tumor resection was successfully visualized through NIR imaging⁸³.

4.5. Polymeric nanoparticles

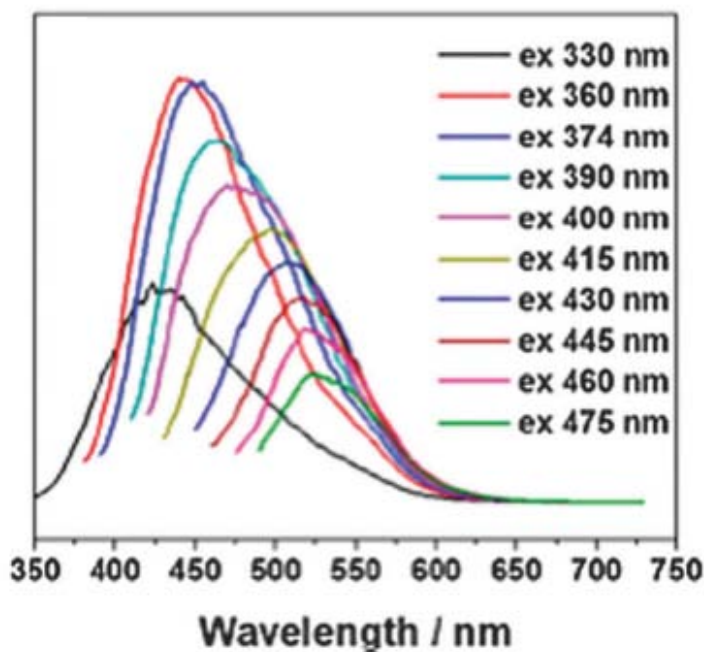


Fig. 11 The excitation wavelengths fluctuation of carbon dots in water (excited at from 330 nm to 475 nm) (reprinted with permission from ref. 84).

Except for the inorganic contrast agents, some dyes also can be used to monitor the pathway of polymeric nanoparticles *in vivo*. For dyes, the precondition in the clinical application for polymeric nanocomposites is penetration to the deep tissue. Therefore, the dyes which can emit far infrared light are first choice as an imaging marker in the construction of theranostic nanocomposites. Wolfbeis et al. systematically reviewed the difference between fluorescent nanomaterials and nanoparticles versus molecular fluorophores, labels and probes in the fluorescent bioimaging. Carbon dots, a cluster of carbon atoms have been used to track the kinetics behavior of nanocomposites *in vivo*. However, the dots with

maximum emission spectra to 650nm has a lower brightness after the penetration into the deep tissues, thus limiting the application in the lab observation and clinical trials (Fig. 11) ⁸⁴.

5. Application of theranostic nanomaterials in diseases

The use of nanomaterials in the delivery of drugs or imaging agents ⁸⁵ has been widely studied. However, the integration of drugs and imaging agents into one type of nanoparticle-based theranostic platform is a new advance in the past decade ⁸⁶. Here, we discuss a wide variety of applications of theranostic nanomaterials in different diseases.

5.1. Cancer

Cancer is one of the most challenging clinical problems and is responsible for approximately 13% of all deaths according to the World Health Organization. The complexity of cancer is a major hurdle in the treatment of the disease. Although prognosis is improving, the large variety of cancers and metastases makes treatment very difficult. Regardless of the treatment method, surgery or chemotherapy, visualization of resection or drug transport in the body will reduce relapse and improve the efficacy of chemotherapeutics ⁸⁷. Recently, the development of nanoscale theranostic platforms has facilitated the above goals.

Magnetic direction is feasible for targeted drug delivery with the aid of superparamagnetic and magnetic susceptibility. Magnetic nanoparticles can improve the outcomes of clinic therapy and enhance brain tumor-targeted drug delivery. EGFR is highly present within glioblastoma (GBM) tumors. And it may be a promising target for imaging and therapeutic purposes ⁸⁸. The wild-type EGFR protein constitutes up to 54% of GBM tumors, while co-overexpression of the wild-type EGFR and its receptor variant III (EGFRvIII) constitutes up to 31% ⁸⁹. The specific antibody-modified iron oxide nanoparticles

(IONPs) can selectively bind to EGFRvIII on human glioblastoma multiforme (GBM) cells⁹⁰. Glioblastoma cell survival was significantly reduced after administration without significant toxicity to human astrocytes. The level of EGFR phosphorylation was reduced in glioblastoma cells after EGFRvIIIAb-IONP treatment. Convection-enhanced delivery (CED) of EGFRvIIIAb-IONPs directed by MRI promoted the initial distribution of IONPs within or adjacent to the intracranial human xenograft tumors and secondary entry into tumor tissues the following day. CED of magnetic nanoparticles significantly improved the survival of animals that were implanted with the glioblastoma xenografts. IONPs connected with high-affinity antibodies specific to the EGFRvIII-knockout mutant were able to selectively enhance MRI contrast and accumulated in the infiltrative glioblastoma cells after CED⁹⁰.

Curcumin and bortezomib can inhibit the growth of cancer cells with a synergistic effect but have no anti-osteoclastogenic activity when combined with alendronate (Aln). However, *in vivo* bioimaging showed that Aln-coated nanoparticles entered bone more easily compared with control groups, promoting bone resorption and inhibiting tumor growth. GNS can offer a stable microenvironment of biomolecules and retain their bioactivity⁹¹. They are currently being studied for drug delivery to pancreatic cancer cells⁹². GNS-based nanomedicine was named CYT-6091 and was used and observed in advanced cancer patients⁹³. The results confirmed that GNS-based nanoparticles were able to significantly reduce the systemic toxicity of chemotherapeutics, an effect that may have been due to the inhibition of an off-target delivery. Eck *et al.* prepared GNS linked to a heterobifunctional PEG that were conjugated with monoclonal antibodies (mAb F19) to label tumor stroma in thin sections of resected pancreatic adenocarcinoma⁹⁴ (Fig. 12). Such antibody-conjugated nanoparticles can be used to image pancreatic cancer stroma through selective interaction with fibroblast activation protein (FAP). The images featured the tissues in dark field microscopy. This theranostic platform may be subjected to clinical application to detect the micrometastasis of pancreatic cancer during surgery.

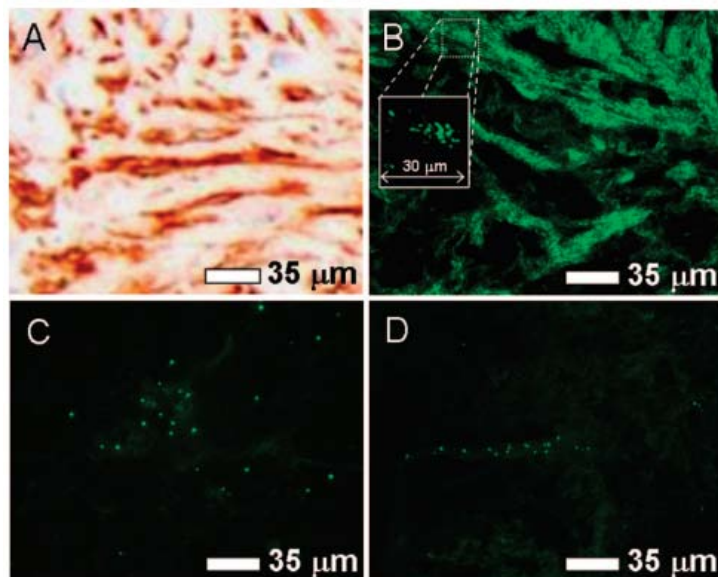


Fig. 12 (A) Representative image of pancreatic cancer tissue (PCT) obtained using immunohistochemistry staining. (B) PCT marked by gold nanoparticles (GNS) modified with monoclonal antibody mAb F19 (GNS-F19); (C) GNS-F19 localization of healthy tissue by using dark-field microscopy; and (D) PCT marked by GNS-mIgG marker (reprinted with permission from ref. 94).

5.2. Cardiovascular diseases

Cardiovascular diseases (CVDs) encompass a series of conditions, involving vasculature and the heart. Generally speaking, when referring to CVDs, atherosclerotic vascular disease and its sequelae, including myocardial infarction and stroke, are implied⁹⁵. Theranostic strategies for atherosclerotic diseases should significantly improve the therapy of cardiovascular conditions. IONPs have been widely used for imaging applications⁵⁹. This application is very important in atherosclerosis therapy as atherosclerosis is difficult to detect before the presence of clinical symptoms⁹⁶.

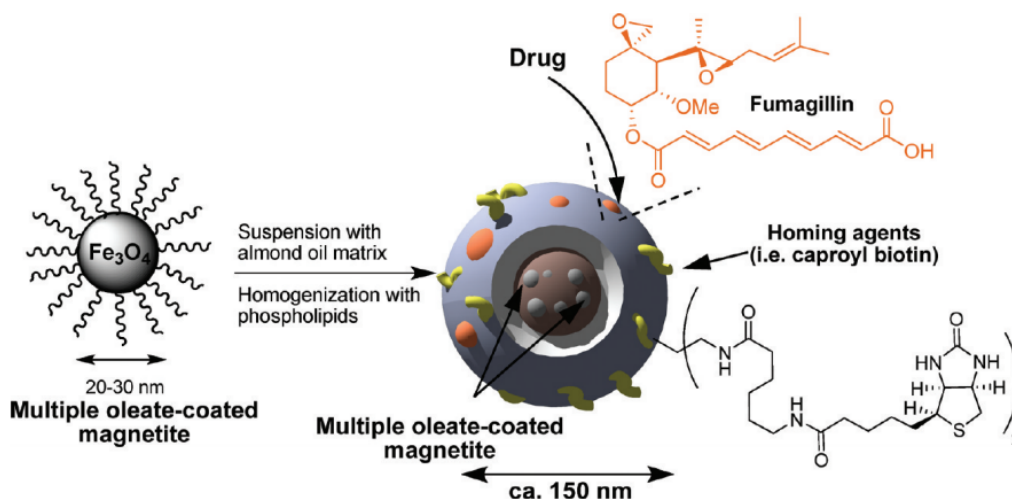


Fig. 13 Schematic illustration of preparation of T1-weighted (T1w) theranostic CION (reprinted with permission from ref. 98).

Lanza's group reported a T1 relaxation effects -weighted (T1w) colloidal iron oxide nanoparticle (CION). This nanoparticle was a cross-linked phospholipid nanoemulsion loaded with oleate-coated magnetite particles. The nanoemulsion reduced T2 relaxation effects, which significant improved positive T1w contrast detection at the nanomolar level⁹⁷. Fumagillin was also loaded into the emulsions containing CIONs⁹⁸ (Fig. 13). Compared with gadolinium, CIONs could effectively reduce T2 relaxation times and enhance negative contrast. Surprisingly, when CIONs coated with oleic acid were dispersed into almond oil and then entrapped by a mixture of phospholipid surfactants, the effect of T2 was reduced, and these nanoparticles became a highly sensitive T1w contrast agent.

Lopez's group⁹⁹ prepared liposomes that recruited activated macrophages because of the metabolically active components from the atheroma tissue. The negatively charged liposomes were loaded with dye (rhodamine), GNS, and lipoprotein-associated phospholipase A2 (LAPA-2). LAPA-2 is an inflammatory biomarker that is highly expressed on activated macrophages. The group confirmed that a high accumulation of liposomes was observed in the shoulder regions of the plaque. They also used transmission electron microscopy to image the localization of lipid vesicles within the atheromas by

detecting the GNS. These results supported that the liposomes conjugated with lipoprotein-associated phospholipase A2 can target the metabolically active regions of plaques.

5.3. Kidney diseases

Because the kidneys can quickly eliminate particles that are smaller than 10 nm in diameter, it is a candidate organ for the targeted delivery of NPs¹⁰⁰. However, the kidney cannot excrete a particle with a diameter of greater than 11 nm because of its anatomical structure¹⁰¹. Many kidney diseases such as acute renal failure (ARF) and chronic kidney disease (CKD) can be treated by NPs.

For life-threatening ARF, dendrimer NP-based MRI techniques can improve disease detection¹⁰². When dendrimers were used to detect ischemia in mice, the data confirmed that the minor increase in the tissue range of the kidney was correlated with the time of ischemia and reperfusion¹⁰³ (Fig. 14). In sepsis-induced ARF models, studies have confirmed that dendrimers loaded with contrast NPs could detect kidney injury by MRI before the elevation of serum creatinine¹⁰⁴. This may help eliminate the nephrotoxic elements before kidney damage is detectable in serum. Haick *et al.* used a non-invasive means to detect end-stage "renal disease" using carbon nanotube in a rat model¹⁰⁵. Work was further performed to identify early-stage CKD by using gold NP sensors. Some genetic diseases may cause the development of renal cysts. Mutations in polycystic kidney disease 1 (PKD1) or PKD2 lead to autosomal dominant PKD (ADPKD) in adults clinically. Europium and terbium phosphors were mixed with gadolinium coated on a magnetic core. These theranostic platforms provided strong luminescence and feasibility of magnetic manipulations in the detection of human ADPKD and other genetic diseases¹⁰⁶.

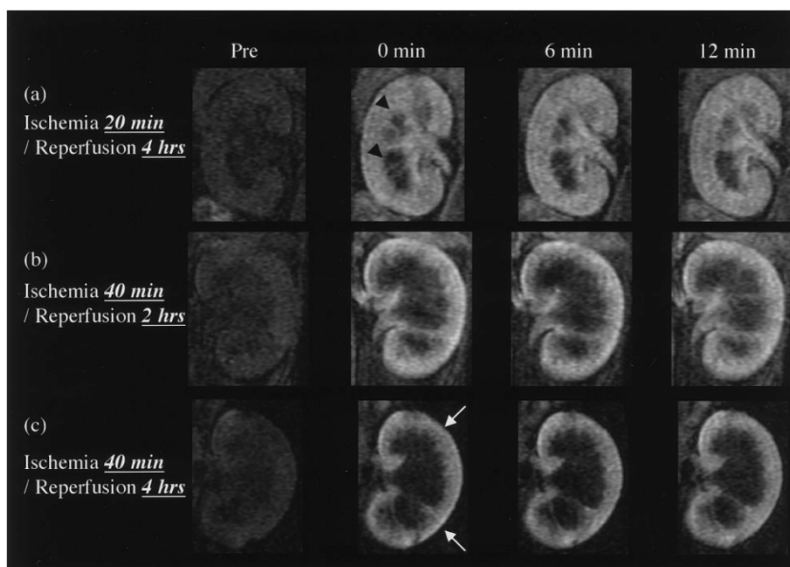


Fig. 14 The micro-MRI of right kidney center with acute ischemic/reperfusion-induced tubular damage (coronal high-resolution images). Time: pre-injection or 0, 6, and 12 min after administration of the diaminobutan polypropylenimine diaminobutyl (DAB)-generation 2 dendrimer (0.03 mmol/kg) (reprinted with permission from ref. 103).

5.4. Pulmonary diseases

Although the alveoli are very small, together they offer a large total surface area for efficient gas exchange, with a single epithelial cell layer separating air from the capillaries. Meanwhile, the huge surface area can also be used to absorb drugs, nanoparticles, and theranostic agents¹⁰⁷.

Apurva *et al.* prepared theranostic nanoparticles from DIM-CpPhC6H5 (DIM-P) conjugated with a PEGylated CREKA peptide targeting lung cancer and investigated the *in vivo* anti-tumor activity. Imaging techniques were used to analyze targeting efficiency. DIM-CpPhC6H5 encapsulated nanoparticles (NCs-D) consisted of lipids and 1,2-dioleoyl-sn-glycero-3-[[N-(5-amino-1-carboxypentyl)iminodiacetic acid] succinyl}(nickel salt) (DOGS-NTA-Ni). These NCs-Ds were coated with PEGylated CREKA peptides which had a stronger binding ability to plasma proteins and stronger inhibition of tumor growth than NCs-D. *In vivo* imaging confirmed that the migration of PEGylated CREKA peptides in the cancer tissue vasculature was 40 times higher than that of NCs-D. The studies demonstrated that the

surface of NCs-D conjugated with PEGylated CREKA peptide (PCNCs-D) constitute a promising theranostic formulation for lung cancer treatment¹⁰⁸ (Fig. 15). Vij *et al.* mixed therapeutics and molecular probes into a matrix of poly (ethylene glycol)-poly(lactic-co-glycolic acid) (PEG-PLGA) to prepare multifunctional polymeric nanoparticles to treat obstructive lung diseases. Recently, non-invasive imaging methods were used to track the distribution and clinic efficacy of nanoparticles in real time for chronic obstructive pulmonary disease (COPD)¹⁰⁹.

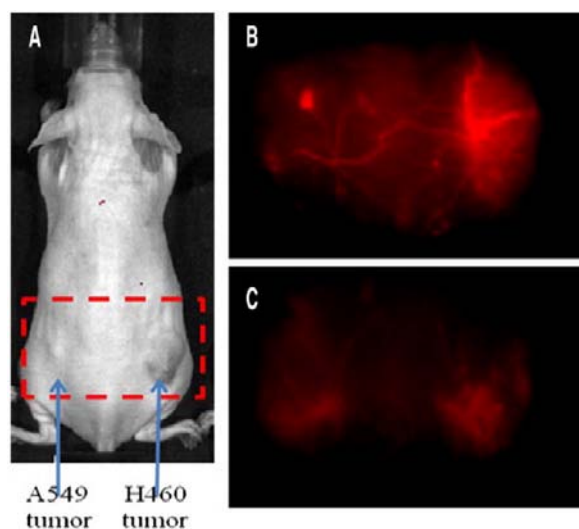


Fig. 15 *In vivo* Image of tumor-bearing mice. (A) A549 (left) and H460 (right) lung tumor cells; (B) PEGylated CREKA peptides targeting vessels, and (C) non-targeted vessels (reprinted with permission from ref. 108).

5.5. Inflammatory diseases

Inflammatory diseases are involved in the activation of cellular immune response. Macrophages internalize nanoparticles and home to the foci of inflammatory tissues in diseases such as rheumatoid arthritis (RA) and multiple sclerosis (MS)¹¹⁰. Macrophages as target cells uptake particles from blood for RA therapy. Researchers have designed RGD-conjugated Au half-shells loaded with methotrexate (MTX) to treat RA. MTX is a first line drug that has been widely used for the treatment of RA¹¹¹. Heat was

locally generated by Au half-shells by near-infrared (NIR) irradiation, resulting in enhanced drug release rates and offering thermal therapy and drug treatment to the inflamed joints simultaneously¹¹² (Fig. 16).

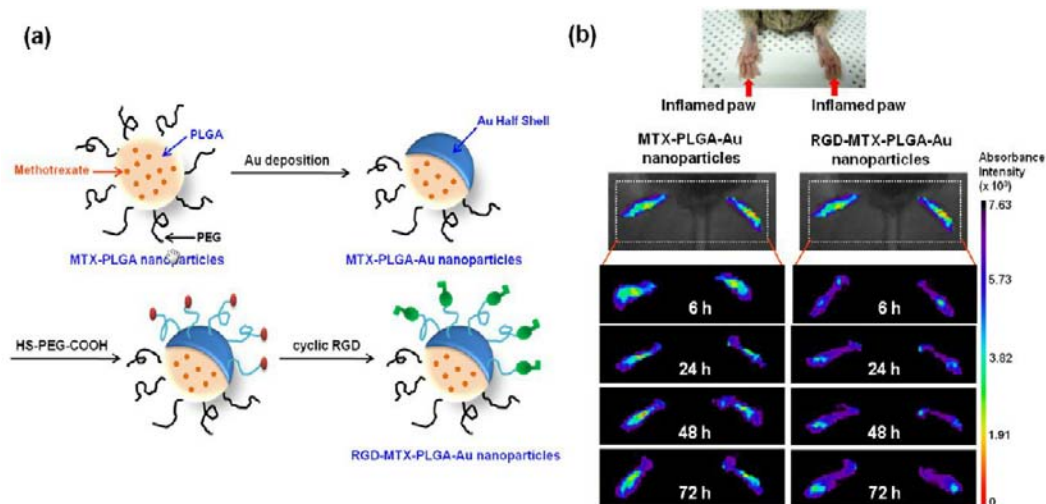


Fig. 16 (a) Schematic illustration of RGD-methotrexate-PLGA-Au nanoshell preparation. (b) NIR images of inflammatory paws of the collagen-induced arthritis (CIA) mice confirmed the dynamics of nanoshells at various time points (6, 24, 48, and 72 h) after injection of methotrexate-PLGA-Au nanoshells (left) or RGD-methotrexate-PLGA-Au nanoshells (right) (reprinted with permission from ref. 112).

5.6. Neurodegenerative diseases

Neurodegenerative disorders (NDs) such as Parkinson's disease and Alzheimer's disease are characterized with progressive loss of neurons' function and structure¹¹³. The blood-brain barrier is the main obstacles to prevent the entry of drugs, nanoparticles, and theranostic agents. Certainly, vascular lesions and leakiness of the BBB may provide an opportunity for the penetration of foreign substances into cerebral parenchyma.

Jason *et al.* confirmed that very small superparamagnetic iron oxide particles (SIOP) can detect lesions in the central nervous system in MS animal models, which cannot be achieved by common MRI contrast agents¹¹⁴. Amiri also summarized the advance of magnetic nanoparticles and SIOP as a theranostic system for Alzheimer's disease¹¹⁵.

6. Clinical trials and the commercial market

Polymeric particulate surfaces provide extensive opportunities for the functionalization of drug delivery systems^{116, 117}. Multimodal conjugated approaches to the treatment and diagnosis of diseases could improve the efficacy and specificity of treatment regimes. Currently, some nanoscale drug delivery systems such as doxorubicin liposomes (DOXIL Injection) and cytarabine/daunorubicin liposomes (CPX-531 formulation) have entered clinical trials as well as commercial markets¹¹⁸⁻¹²⁰. Although nanoscale theranostic platforms can deliver active therapeutics and imaging agents, no currently available products can be used for the treatment of patients. On the clinical side, Stanley *et al.* studied the influence of 68-Ga-THERANOSTIC, an $\alpha v\beta 3$ integrin antagonist, on non-small lung cancer and breast cancer by using PET/CT. The data confirmed that compared with Ga, there were many virtues such as safety, effectiveness, high tolerance, low irradiation, and convenient labeling, which warranted this platform for further clinical trials¹²¹. In another study, PLGA-Au half-shell nanoparticles designed by Park *et al.* will be tested in phase I clinical trials because of their higher therapeutic efficiency caused by the synergistic effects of chemotherapeutics and thermotherapy¹²². As the first theranostic platform, polymeric HPMA-Doxorubicin conjugates labeled with ¹³¹I have translated into phase I clinical trial¹²³. Hopefully, theranostic formulations based on real-time detectable signals, positively related to the severity of various diseases, can eventually meet the growth requirements in the field of individual therapy in the future¹²⁴.

7. Conclusion and prospect

Theranostic platforms based on nanomaterials are an emerging area of research integrating targeted delivery and local imaging for diagnosis, which further directs the operation of surgery. Because of the inheritance of techniques from targeted drug delivery, many strategies have been syncretized, such as surface modification, loading process, and tracking drugs in local tissues, which are similar to the loading of therapeutics in nanomaterials. However, there are some differences between loading and tracking due to the combination and properties of the drug and tracking reagents, such as solubility, polarity,

sensitivity to oxide, pH condition, humidity, and light. A reasonable fabrication process and loading method should be selected for the protection of drug efficacy and the signal of the imaging reagent. For tracking of imaging agent, the big challenge is to improve the metabolism and decrease the deposition of inorganic materials in the body. Meanwhile, the sensitivity of signal determines the following application of the resulted theranostics in the clinics. The therapeutic effect is based on the targeting efficiency and effective drug accumulation; the diagnostic sensitivity is determined by the type and loading efficiency of bioimaging agent. In addition, unbeneficial interactions of drug chemicals with imaging molecules, such as the complexation, chelation, dye quenching, and drug toxicity, should be avoided. On the other hand, the integration of theranostic platforms should place signal tracking, therapeutic efficacy, and synergistic effects into first priority. Certainly, efforts may need to be made at the end point to achieve specific aims, such as the removal of tumors and localization of thrombi. Researchers should also consider the compatibility of drugs and signal substances, preparation cost, equipment design, and feasibility of industrialization. Meanwhile, the penetration of signal from deep tissues and the discrimination between healthy and abnormal cells would influence the development of theranostic platforms. The chronic toxicity of unspecific drug accumulation and the metabolism of metal particles and fluorescent dyes would encumber clinical applications after translation^{125, 126}. Evidently, there is still a long way to go before we can achieve a practical theranostic system based on polymeric multifunctional nanomaterials.

Acknowledgments

This work was supported by Iowa State University (ISU) President's Initiative on Interdisciplinary Research (PIIR) program, Cyclone Research Partnership Grant, McGee-Wagner Interdisciplinary Research Foundation, and the grant from the project of Heilongjiang Provincial Education Bureau Foundation (12511322).

Reference:

1. G. J. Sumer B, *Nanomedicine (Lond)*, 2008, 3, 137-140.
2. H. Shelanski and M. Shelanski, *The Journal of the International College of Surgeons*, 1956, 25, 727.
3. H. A. Ravin, A. M. Seligman and J. Fine, *New England Journal of Medicine*, 1952, 247, 921-929.
4. M. S. Muthu, D. T. Leong, L. Mei and S. S. Feng, *Theranostics*, 2014, 4, 660-677.
5. M. Liu, M. Li, G. Wang, X. Liu, D. Liu, H. Peng and Q. Wang, *Journal of Biomedical Nanotechnology*, 2014, 10, 2038-2062.
6. F. Ding, H. Deng, Y. Du, X. Shi and Q. Wang, *Nanoscale*, 2014, 6, 9477-9493.
7. M. Li, H. Deng, H. Peng and Q. Wang, *Journal of nanoscience and nanotechnology*, 2014, 14, 415-432.
8. J. Li, M. M. Cona, F. Chen, Y. Feng, L. Zhou, G. Zhang, J. Nuyts, P. de Witte, J. Zhang and J. Yu, *Theranostics*, 2013, 3, 127.
9. L. Jing, X. Liang, X. Li, L. Lin, Y. Yang, X. Yue and Z. Dai, *Theranostics*, 2014, 4, 858.
10. S. M. Janib, A. S. Moses and J. A. MacKay, *Adv Drug Deliv Rev*, 2010, 62, 1052-1063.
11. M. K. Yu, J. Park and S. Jon, *Theranostics*, 2012, 2, 3-44.
12. J. Xie, S. Lee and X. Chen, *Adv Drug Deliv Rev*, 2010, 62, 1064-1079.
13. F. Jia, X. Liu, L. Li, S. Mallapragada, B. Narasimhan and Q. Wang, *Journal of Controlled Release*, 2013, 172, 1020-1034.
14. S.-S. Feng, 2006.
15. M. S. Muthu and S.-S. Feng, *Expert opinion on drug delivery*, 2013, 10, 151-155.
16. M. S. Muthu and S. Singh, 2009.
17. M. E. Calderera-Moore, W. B. Liechty and N. A. Peppas, *Acc Chem Res*, 2011, 44, 1061-1070.
18. S. P. Newman and I. R. Wilding, *Pharmaceutical science & technology today*, 1999, 2, 181-189.
19. M. Calderera-Moore and N. A. Peppas, *Adv Drug Deliv Rev*, 2009, 61, 1391-1401.
20. W. B. Liechty, D. R. Kryscio, B. V. Slaughter and N. A. Peppas, *Annu Rev Chem Biomol Eng*, 2010, 1, 149.
21. H. Ding and F. Wu, *Theranostics*, 2012, 2, 1040.
22. I. Velikyan, *Theranostics*, 2012, 2, 424.
23. J. Yuan, H. Zhang, H. Kaur, D. Oupicky and F. Peng, *Molecular imaging*, 2012, 12, 203-212.
24. B. Zarabi, M. P. Borgman, J. Zhuo, R. Gullapalli and H. Ghandehari, *Pharm Res*, 2009, 26, 1121-1129.
25. A. Mitra, J. Mulholland, A. Nan, E. McNeill, H. Ghandehari and B. R. Line, *Journal of Controlled Release*, 2005, 102, 191-201.
26. B. R. Line, A. Mitra, A. Nan and H. Ghandehari, *Journal of Nuclear Medicine*, 2005, 46, 1552-1560.
27. F. Ye, T. Ke, E.-K. Jeong, X. Wang, Y. Sun, M. Johnson and Z.-R. Lu, *Mol Pharm*, 2006, 3, 507-515.
28. J. Ye, Q. Wang, X. Zhou and N. Zhang, *International journal of pharmaceuticals*, 2008, 352, 273-279.
29. R. Bi, W. Shao, Q. Wang and N. Zhang, *Journal of Biomedical Nanotechnology*, 2009, 5, 84-92.
30. P. Ekambaram, A. A. H. Sathali and K. Priyanka, *Sci Rev Chem Commun*, 2012, 2, 80-102.
31. H. Chen, X. Chang, D. Du, W. Liu, J. Liu, T. Weng, Y. Yang, H. Xu and X. Yang, *Journal of Controlled Release*, 2006, 110, 296-306.
32. P. V. Pople and K. K. Singh, *Aaps Pharmscitech*, 2006, 7, E63-E69.

33. B. Sarmiento, S. Martins, D. Ferreira and E. B. Souto, *International journal of nanomedicine*, 2007, 2, 743.
34. A. Silva, E. González-Mira, M. García, M. Egea, J. Fonseca, R. Silva, D. Santos, E. Souto and D. Ferreira, *Colloids and Surfaces B: Biointerfaces*, 2011, 86, 158-165.
35. C. Charcosset, A. El-Harati and H. Fessi, *Journal of Controlled Release*, 2005, 108, 112-120.
36. A. Ahmed El-Harati, C. Charcosset and H. Fessi, *Pharmaceutical development and technology*, 2006, 11, 153-157.
37. I. Singh, R. Swami, W. Khan and R. Sistla, *Expert opinion on drug delivery*, 2014, 11, 211-229.
38. L. Harivardhan Reddy, R. Sharma, K. Chuttani, A. Mishra and R. Murthy, *Journal of Controlled Release*, 2005, 105, 185-198.
39. R. Cavalli, G. P. Zara, O. Caputo, A. Bargoni, A. Fundarò and M. R. Gasco, *Pharmacological research*, 2000, 42, 541-545.
40. K. H. Bae, J. Y. Lee, S. H. Lee, T. G. Park and Y. S. Nam, *Adv Healthc Mater*, 2013, 2, 576-584.
41. E. R. Gillies and J. M. Frechet, *Drug Discov Today*, 2005, 10, 35-43.
42. G. J. Kirkpatrick, J. A. Plumb, O. B. Sutcliffe, D. J. Flint and N. J. Wheate, *Journal of inorganic biochemistry*, 2011, 105, 1115-1122.
43. C. Ornelas, R. Pennell, L. F. Liebes and M. Weck, *Organic letters*, 2011, 13, 976-979.
44. O. Taratula, C. Schumann, M. A. Naleway, A. J. Pang, K. J. Chon and O. Taratula, *Mol Pharm*, 2013, 10, 3946-3958.
45. G. K. Grünwald, A. Vetter, K. Klutz, M. J. Willhauck, N. Schwenk, R. Senekowitsch-Schmidtke, M. Schwaiger, C. Zach, E. Wagner and B. Göke, *Molecular Therapy—Nucleic Acids*, 2013, 2, e131.
46. M. S. Muthu and S.-S. Feng, *Nanomedicine*, 2010, 5, 1017-1019.
47. C. Grange, S. Geninatti-Crich, G. Esposito, D. Alberti, L. Tei, B. Bussolati, S. Aime and G. Camussi, *Cancer Res*, 2010, 70, 2180-2190.
48. R. Bi, W. Shao, Q. Wang and N. Zhang, *Journal of drug targeting*, 2008, 16, 639-648.
49. M. Liu, M. Li, S. Sun, B. Li, D. Du, J. Sun, F. Cao, H. Li, F. Jia, T. Wang, N. Chang, H. Yu, Q. Wang and H. Peng, *Biomaterials*, 2014, 35, 3697-3707.
50. D. Du, N. Chang, S. Sun, M. Li, H. Yu, M. Liu, X. Liu, G. Wang, H. Li, X. Liu, Q. Wang and H. Peng, *Journal of Controlled Release*, 2014, 182, 99-110.
51. M. Li, H. Yu, T. Wang, N. Chang, J. Zhang, D. Du, M. Liu, S. Sun, R. Wang, H. Tao, Z. Shen, Q. Wang and H. Peng, *Journal of Materials Chemistry B*, 2014, 2, 1619-1625.
52. A. Sharma and U. S. Sharma, *International journal of pharmaceuticals*, 1997, 154, 123-140.
53. J. Agulla, D. Brea, F. Campos, T. Sobrino, B. Argibay, W. Al-Soufi, M. Blanco, J. Castillo and P. Ramos-Cabrer, *Theranostics*, 2014, 4, 90.
54. C.-J. Wen, L.-W. Zhang, S. A. Al-Suwayeh, T.-C. Yen and J.-Y. Fang, *Int J Nanomedicine*, 2012, 7, 1599.
55. K. Kataoka, A. Harada and Y. Nagasaki, *Advanced drug delivery reviews*, 2001, 47, 113-131.
56. Z. Wan, H. Mao, M. Guo, Y. Li, A. Zhu, H. Yang, H. He, J. Shen, L. Zhou and Z. Jiang, *Theranostics*, 2014, 4, 399.
57. Montet X, Funovics M, Montet-Abou K, Weissleder R and J.-s. L., *J Med Chem*, 2006, 6087-6093.
58. B. T. Luk, R. H. Fang and L. Zhang, *Theranostics*, 2012, 2, 1117-1126.
59. A. K. Gupta and M. Gupta, *Biomaterials*, 2005, 26, 3995-4021.
60. S. K. Yen, P. Padmanabhan and S. T. Selvan, *Theranostics*, 2013, 3, 986-1003.
61. Veiseh O, G. J. Sun C, Kohler N, Gabikian P, Lee D, Bhattarai N, Ellenbogen R, Sze R, Hallahan A, Olson J and Z. M., *Nano Lett* 2005, 5, 1003-1008.
62. T. J. Chen, T. H. Cheng, Y. C. Hung, K. T. Lin, G. C. Liu and Y. M. Wang, *Journal of biomedical materials research Part A*, 2008, 87, 165-175.

63. Lee H, Lee E, Kim DK, Jang NK, Jeong YY and J. S., *J. Am. Chem. Soc.*, 2006, 128, 7383-7389.
64. E. Valero, S. Tambalo, P. Marzola, M. Ortega-Munoz, F. J. Lopez-Jaramillo, F. Santoyo-Gonzalez, J. de Dios Lopez, J. J. Delgado, J. J. Calvino, R. Cuesta, J. M. Dominguez-Vera and N. Galvez, *J Am Chem Soc*, 2011, 133, 4889-4895.
65. H. Xu, Z. P. Aguilar, L. Yang, M. Kuang, H. Duan, Y. Xiong, H. Wei and A. Wang, *Biomaterials*, 2011, 32, 9758-9765.
66. Smith JE, Medley CD, Tang Z, Shangguan D, Lofton C and T. W., *Anal. Chem.*, 2007, 79, 3075-3082.
67. Y. Ling, K. Wei, Y. Luo, X. Gao and S. Zhong, *Biomaterials*, 2011, 32, 7139-7150.
68. Wenthe MN, Jain A, Kono E, Berberat PO, Giese T and Reber HA, *Pancreas* 2005, 31, 119-125.
69. B. Moulari, D. Pertuit, Y. Pellequer and A. Lamprecht, *Biomaterials*, 2008, 29, 4554-4560.
70. V. Mamaeva, J. M. Rosenholm, L. T. Bate-Eya, L. Bergman, E. Peuhu, A. Duchanoy, L. E. Fortelius, S. Landor, D. M. Toivola, M. Linden and C. Sahlgren, *Mol Ther*, 2011, 19, 1538-1546.
71. B. Zhao, J. J. Yin, P. J. Bilski, C. F. Chignell, J. E. Roberts and Y. Y. He, *Toxicol Appl Pharmacol*, 2009, 241, 163-172.
72. G. Plascencia-Villa, D. Bahena, A. R. Rodriguez, A. Ponce and M. Jose-Yacaman, *Metallomics*, 2013, 5, 242-250.
73. R. Kumar, H. Korideck, W. Ngwa, R. I. Berbeco, G. M. Makrigiorgos and S. Sridhar, *Transl Cancer Res*, 2013, 2.
74. H. Chen, X. Zhang, S. Dai, Y. Ma, S. Cui, S. Achilefu and Y. Gu, *Theranostics*, 2013, 3, 633-649.
75. W. Lu, A. K. Singh, S. A. Khan, D. Senapati, H. Yu and P. C. Ray, *Journal of the American Chemical Society*, 2010, 132, 18103-18114.
76. J. Li, S. Gupta and C. Li, *Quant Imaging Med Surg*, 2013, 3, 284-291.
77. D. N. Heo, D. H. Yang, H. J. Moon, J. B. Lee, M. S. Bae, S. C. Lee, W. J. Lee, I. C. Sun and I. K. Kwon, *Biomaterials*, 2012, 33, 856-866.
78. J. Shao, R. J. Griffin, E. I. Galanzha, J. W. Kim, N. Koonce, J. Webber, T. Mustafa, A. S. Biris, D. A. Nedosekin and V. P. Zharov, *Sci Rep*, 2013, 3, 1293.
79. W. C. Chan and S. Nie, *Science*, 1998, 281, 2016-2018.
80. M. E. Akerman, W. C. Chan, P. Laakkonen, S. N. Bhatia and E. Ruoslahti, *Proc Natl Acad Sci U S A*, 2002, 99, 12617-12621.
81. Bagalkot V, Zhang L, Levy-Nissenbaum E, Jon S, Kantoff PW, Langer R and F. OC, *Nano Lett*, 2007, 7, 3065-3070.
82. Y. P. Ho and K. W. Leong, *Nanoscale*, 2010, 2, 60-68.
83. Y. Li, Z. Li, X. Wang, F. Liu, Y. Cheng, B. Zhang and D. Shi, *Theranostics*, 2012, 2, 769-776.
84. O. S. Wolfbeis, *Chemical Society Reviews*, 2015.
85. C. Sun, J. S. Lee and M. Zhang, *Advanced drug delivery reviews*, 2008, 60, 1252-1265.
86. J. Della Rocca, D. Liu and W. Lin, *Accounts of chemical research*, 2011, 44, 957-968.
87. I. Brigger, C. Dubernet and P. Couvreur, *Advanced drug delivery reviews*, 2002, 54, 631-651.
88. M. Wankhede, A. Bouras, M. Kaluzova and C. G. Hadjipanayis, *Expert Rev Clin Pharmacol*, 2012, 5, 173-186.
89. Amy B. Heimberger, Roman Hlatky and D. Suki, *Clin. Cancer Res.*, 2005, 11, 1462-1466.
90. C. G. Hadjipanayis, R. Machaidze, M. Kaluzova, L. Wang, A. J. Schuette, H. Chen, X. Wu and H. Mao, *Cancer Res*, 2010, 70, 6303-6312.
91. M. S. Muthu and S. Singh, *Nanomedicine (Lond)*, 2009, 4, 105-118.
92. C. R. Patra, R. Bhattacharya, E. Wang, A. Katarya, J. S. Lau, S. Dutta, M. Muders, S. Wang, S. A. Buhrow, S. L. Safgren, M. J. Yaszemski, J. M. Reid, M. M. Ames, P. Mukherjee and D. Mukhopadhyay, *Cancer Res*, 2008, 68, 1970-1978.

93. S. K. Libutti, G. F. Paciotti, A. A. Byrnes, H. R. Alexander, Jr., W. E. Gannon, M. Walker, G. D. Seidel, N. Yuldasheva and L. Tamarkin, *Clin Cancer Res*, 2010, 16, 6139-6149.
94. W. Eck, G. Craig, A. Sigdel, G. Ritter, L. J. Old, L. Tang, M. F. Brennan, P. J. Allen and M. D. Mason, *ACS Nano*, 2008, 2, 2263-2272.
95. S. Yusuf, P. Sleight, J. Pogue, J. Bosch, R. Davies and G. Dagenais, *The New England journal of medicine*, 2000, 342, 145-153.
96. V. L. Roger, A. S. Go, D. M. Lloyd-Jones, R. J. Adams, J. D. Berry, T. M. Brown, M. R. Carnethon, S. Dai, G. de Simone, E. S. Ford, C. S. Fox, H. J. Fullerton, C. Gillespie, K. J. Greenlund, S. M. Hailpern, J. A. Heit, P. M. Ho, V. J. Howard, B. M. Kissela, S. J. Kittner, D. T. Lackland, J. H. Lichtman, L. D. Lisabeth, D. M. Makuc, G. M. Marcus, A. Marelli, D. B. Matchar, M. M. McDermott, J. B. Meigs, C. S. Moy, D. Mozaffarian, M. E. Mussolino, G. Nichol, N. P. Paynter, W. D. Rosamond, P. D. Sorlie, R. S. Stafford, T. N. Turan, M. B. Turner, N. D. Wong and J. Wylie-Rosett, *Circulation*, 2011, 123, e18-e209.
97. H. Frank, R. Weissleder and T. J. Brady, *AJR Am J Roentgenol*, 1994, 162, 209-213.
98. A. Senpan, S. D. Caruthers, I. Rhee, N. A. Mauro, D. Pan, G. Hu, M. J. Scott, R. W. Fuhrhop, P. J. Gaffney, S. A. Wickline and G. M. Lanza, *ACS Nano*, 2009, 3, 3917-3926.
99. B. L. Walton, M. Leja, K. C. Vickers, M. Estevez-Fernandez, A. Sanguino, E. Wang, F. J. Clubb, Jr., J. Morrisett and G. Lopez-Berestein, *Vasc Med*, 2010, 15, 307-313.
100. Choi CH, Zuckerman JE, Webster P and D. ME, *Proc Natl Acad Sci*, 2011, 108, 6656-6661.
101. P. L. Choyke and H. Kobayashi, *Abdom Imaging*, 2006, 31, 224-231.
102. S. Uchino, J. A. Kellum, R. Bellomo, G. S. Doig, H. Morimatsu, S. Morgera, M. Schetz, I. Tan, C. Bouman, E. Macedo, N. Gibney, A. Tolwani and C. Ronco, *JAMA*, 2005, 294, 813-818.
103. H. Kobayashi, S. K. Jo, S. Kawamoto, H. Yasuda, X. Hu, M. V. Knopp, M. W. Brechbiel, P. L. Choyke and R. A. Star, *J Magn Reson Imaging*, 2004, 20, 512-518.
104. J. W. Dear, H. Kobayashi, M. W. Brechbiel and R. A. Star, *Nephron Clin Pract*, 2006, 103, c45-49.
105. H. Haick, M. Hakim, M. Patrascu, C. Levenberg, N. Shehada, F. Nakhoul and Z. Abassi, *ACS Nano*, 2009, 3, 1258-1266.
106. A. Son, A. Dhirapong, D. K. Dosev, I. M. Kennedy, R. H. Weiss and K. R. Hristova, *Anal Bioanal Chem*, 2008, 390, 1829-1835.
107. M. Howell, C. Wang, A. Mahmoud, G. Hellermann, S. S. Mohapatra and S. Mohapatra, *Drug Delivery and Translational Research*, 2013, 3, 352-363.
108. A. R. Patel, M. B. Chougule, E. Lim, K. P. Francis, S. Safe and M. Singh, *Nanomedicine: Nanotechnology, Biology and Medicine*, 2013, DOI: 10.1016/j.nano.2013.12.002.
109. N. Vij, *Expert Opin Drug Deliv*, 2011, 8, 1105-1109.
110. W. Ulbrich and A. Lamprecht, *J R Soc Interface*, 2010, 7 Suppl 1, S55-66.
111. R. Maini, E. W. St Clair, F. Breedveld, D. Furst, J. Kalden, M. Weisman, J. Smolen, P. Emery, G. Harriman and M. Feldmann, *The Lancet*, 1999, 354, 1932-1939.
112. S. M. Lee, H. J. Kim, Y. J. Ha, Y. N. Park, S. K. Lee, Y. B. Park and K. H. Yoo, *ACS Nano*, 2013, 7, 50-57.
113. F. Re, M. Gregori and M. Masserini, *Nanomedicine*, 2012, 8 Suppl 1, S51-58.
114. J. M. Millward, J. Schnorr, M. Taupitz, S. Wagner, J. T. Wuerfel and C. Infante-Duarte, *ASN Neuro*, 2013, 5, e00110.
115. H. Amiri, K. Saeidi, P. Borhani, A. Manafirad, M. Ghavami and V. Zerbi, *ACS chemical neuroscience*, 2013, 4, 1417-1429.
116. Z. Gu, A. A. Aimetti, Q. Wang, T. T. Dang, Y. Zhang, O. Veisoh, H. Cheng, R. S. Langer and D. G. Anderson, *ACS nano*, 2013, 7, 4194-4201.

117. B. Büyüktimkin, Q. Wang, P. Kiptoo, J. M. Stewart, C. Berkland and T. J. Siahaan, *Molecular pharmaceuticals*, 2012, 9, 979-985.
118. E. Miele, G. P. Spinelli, E. Miele, F. Tomao and S. Tomao, *Int J Nanomedicine*, 2009, 4, 99.
119. Y. Malam, M. Loizidou and A. M. Seifalian, *Trends in pharmacological sciences*, 2009, 30, 592-599.
120. P. Tardi, S. Johnstone, N. Harasym, S. Xie, T. Harasym, N. Zisman, P. Harvie, D. Bermudes and L. Mayer, *Leukemia research*, 2009, 33, 129-139.
121. S. Satz, R. Baum, H. Kulkarni, D. Narasimhan, D. Mueller, M. Brechbiel and Y.-S. Kim, 2014.
122. H. Park, J. Yang, J. Lee, S. Haam, I.-H. Choi and K.-H. Yoo, *ACS Nano*, 2009, 3, 2919-2926.
123. P. A. Vasey, S. B. Kaye, R. Morrison, C. Twelves, P. Wilson, R. Duncan, A. H. Thomson, L. S. Murray, T. E. Hilditch and T. Murray, *Clinical Cancer Research*, 1999, 5, 83-94.
124. N. Limaye, *Applied & Translational Genomics*, 2013, 2, 17-21.
125. R. F. Minchin and D. J. Martin, *Endocrinology*, 2010, 151, 474-481.
126. C. F. Jones and D. W. Grainger, *Advanced drug delivery reviews*, 2009, 61, 438-456.